[Supplementary Information]

Boosted Thermogalvanic Thermopower upon Solid-to-Liquid Phase Transition

Dongjoon Shin[1†], Kihoon Ryu[2†], Daehyun Kim[1], Eunho Choi[2], Seunghoon Chae[1], Yundong Lee[2], Yong Tae Kang[1], Sangtae Kim[2,3]*, Wonjoon Choi[1]*

1. Department of Mechanical Engineering, Korea University, Seoul, Korea.

2. Department of Nuclear Engineering, Hanyang University, Seoul, Korea.

3. Department of Materials Science and Engineering, Hanyang University, Seoul, Korea.

* Correspondence should be addressed to S. Kim (sangtae@hanyang.ac.kr) and W. Choi (wojchoi@korea.ac.kr)

† These authors contributed equally to this work.

The supplementary information includes:

Fig. S1 to S17
Supplementary Notes

[Table of Contents for Supplementary Information]

between 4 ºC and 14 ºC. The electrode undergoes partial liquid-to-solid phase transition at the solidus temperature around 7 ºC.

Fig. S15 | The measured current and resultant power output of the TGH device according to the external resistance. The thickness of the electrode was 0.64 cm.

Fig. S16 | The measurement setup for thermogalvanic devices with Na-K liquid metal electrodes targeting spatial temperature gradients. In-house thermogalvanic cells with polyethylene body is used with 1x1 cm^2 electrode area.

Fig. S17 | The measurement setup for coin cell-based temporal thermal energy harvesters employing Na-K liquid metal electrodes

Supplementary Note 1 | Thermodynamic model for phase transition-driven thermopower

Supplementary Note 2 | The electrolyte effects on the thermopower measurements

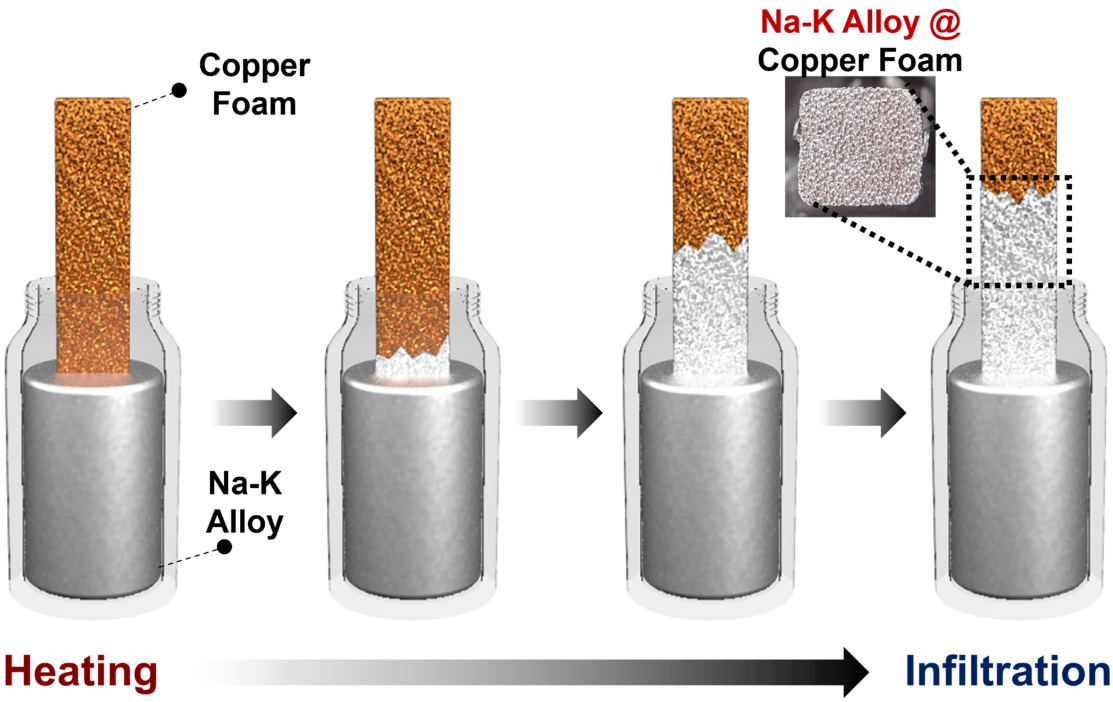

Fig. S1 The fabrication of liquid metal electrodes with Na-K alloys infiltrated in copper foam.

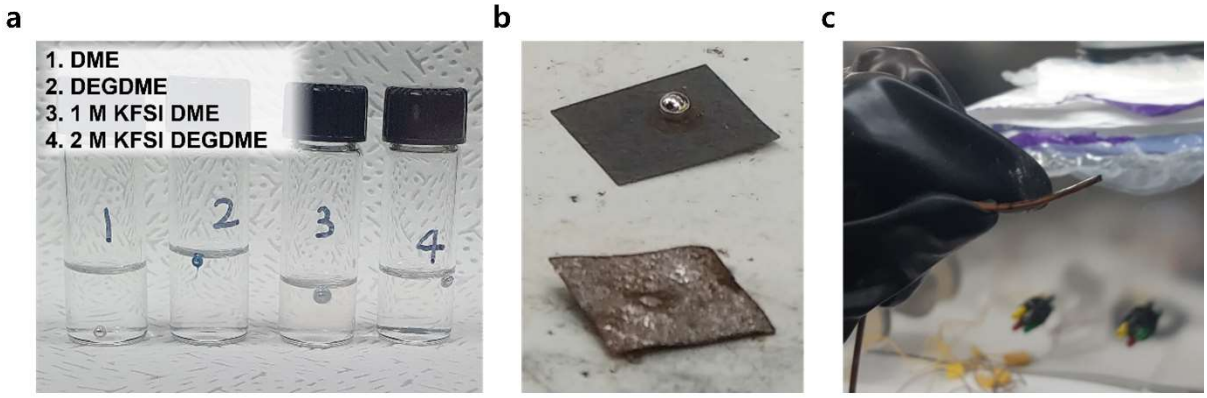

Fig. S2 The instability of Na-K liquid metal electrode. (a) The NaK alloy floats above solvents and K^+ electrolyte due to density difference. (b) infiltration of NaK alloy into carbon paper and NaK infiltrated carbon paper becomes brittle. (c) The high reactivity of NaK alloys contaminates PTFE coated thermocouple.

Note:

Liquid metal electrodes that are too thin may form spherical shapes due to Rayleigh instability and high surface tension. As shown in Fig. S2a, Na-K alloy droplets float in the electrolytes due to their lower density, causing instability if the electrode is very thin. Conversely, very thick electrodes may experience severe curvature changes upon melting. To mitigate these issues, copper foam was used to encapsulate the Na-K alloy, suppressing morphological changes during phase transitions. The resulting electrode thickness was 6.4 mm, providing the necessary bulk volume and stability. As shown in Fig. S2b, carbon-based substrates like carbon cloths and papers were tested and showed better alkali metal wettability than copper foam. However, they became brittle and less durable after wetting, making them unsuitable for our experiments.

All polymer materials touching NaK alloys are composed of oxygen-free polyethylene and polypropylene to prevent potential oxidation of liquid metal alloys. When other polymers containing O or F, such as polytetrafluoroethylene (PTFE) and polyimide are used, they reacted with liquid NaK alloys and led to explosion or severe noise in voltage signals. The chemical reaction between PTFE and NaK alloys was notably explosive, making carbon soot, as seen in Fig. S2C. Additionally, the thermocouple was sheathed by PE to prevent short-circuit and reaction between NaK alloys and thermocouple. Otherwise, it consistently resulted in incorrect voltage or temperature measurements on the potentiostat, multimeter, and thermocouple due to voltage noise.

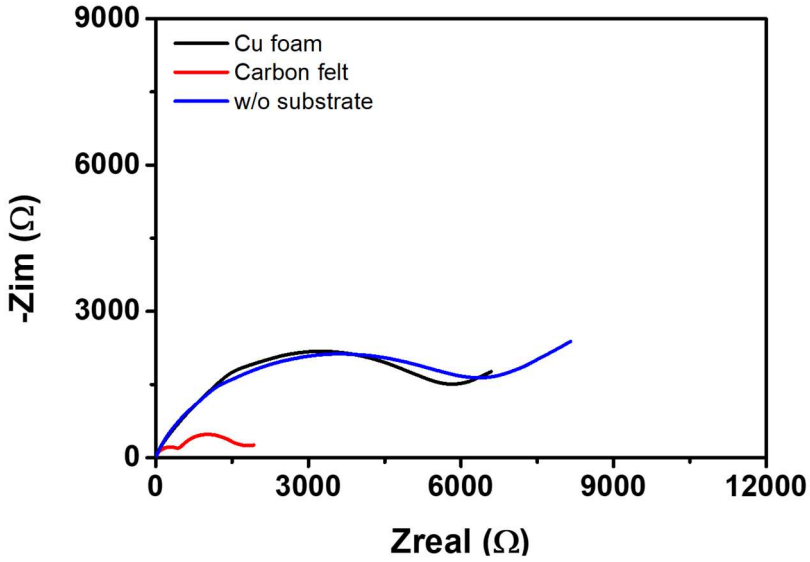

Fig. S3 The electrochemical impedance spectroscopy (EIS) measurements with and without Cu foam and carbon felt.

Note:

The EIS measurements with Cu foam or carbon felt resulted in improved charge transfer resistance compared to bare metal Na_xK alloy. Bare Na_xK alloy was inserted into polyethylene block with 1x1 cm^2 area after cooling to sufficiently low temperature for easy handling. The EIS measurements were performed on in-house thermogalvanic device fabricated with polyethylene blocks. Na_xK alloys inserted in carbon felt exhibits the lowest impedances, yet avoided in active thermogalvanic investigation due to potential interstitial doping of carbon into the alloy. Na_xK alloys inserted in copper foam resulted in only slightly reduced impedance, yet the morphological stability was notably improved during extended experiments longer than 10 hours.

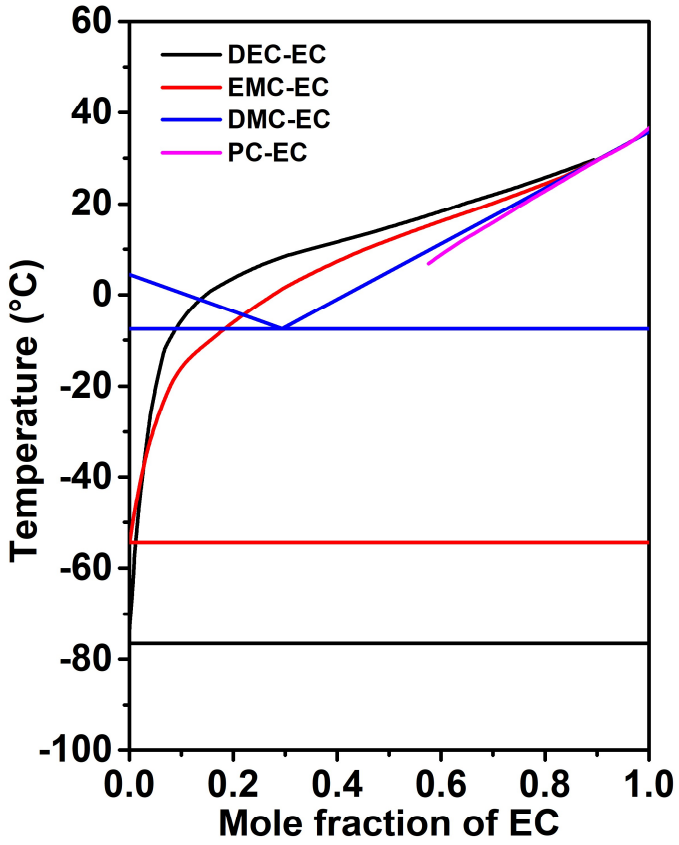

Fig. S4 The eutectic phase diagrams of carbonate-based electrolytes with respect to EC contents.

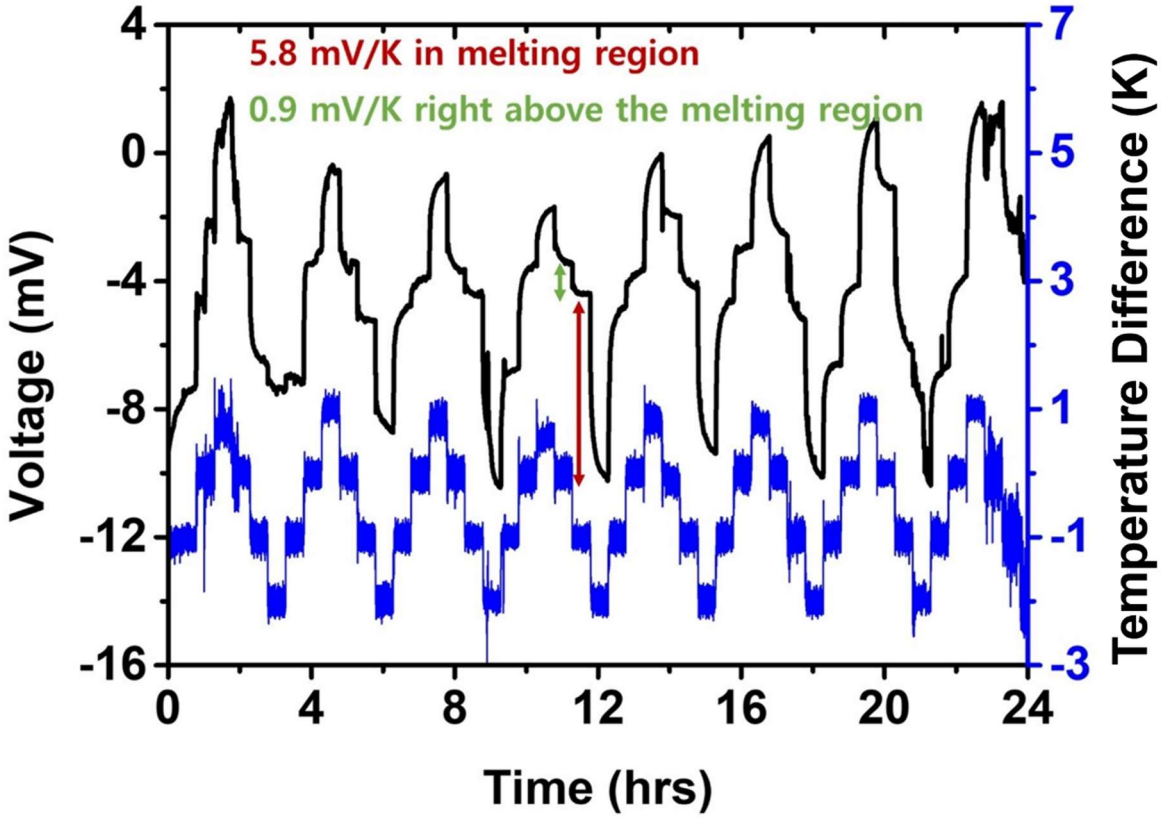

Fig. S5 The differential thermopower measurement upon one Kelvin difference across the thermogalvanic device. The device operating across solidus 6-7 ºC clearly exhibits increased thermopower compared to the temperatures above solidus.

Note:

The experiments were initially prepared at 8 ºC on two identical $Na_{2+x}K$ electrodes. With two-staged Peltier cooler and CPU-grade fans with heat sinks attached to both electrodes, the temperatures on both electrodes were carefully controlled using in-house temperature controller based on a feedback loop coded to an Arduino Uno board. One electrode was maintained at 8 ºC throughout the experiment, and 0 K difference indicates that both electrodes are maintained at 8 ºC. Then, the other electrode was varied in temperature by 1 K, to 9 ºC (+1 K difference in ΔT), 7 ºC (-1 K difference in ΔT) and 6 ºC (-2 K difference in ΔT). The measured voltage changes indicate the voltage changes associated with each 1 K temperature change interval. We clearly observe notably high voltage difference during the temperature change from 7 ºC to 6 ºC, demonstrating phase transition-driven thermo-voltage.

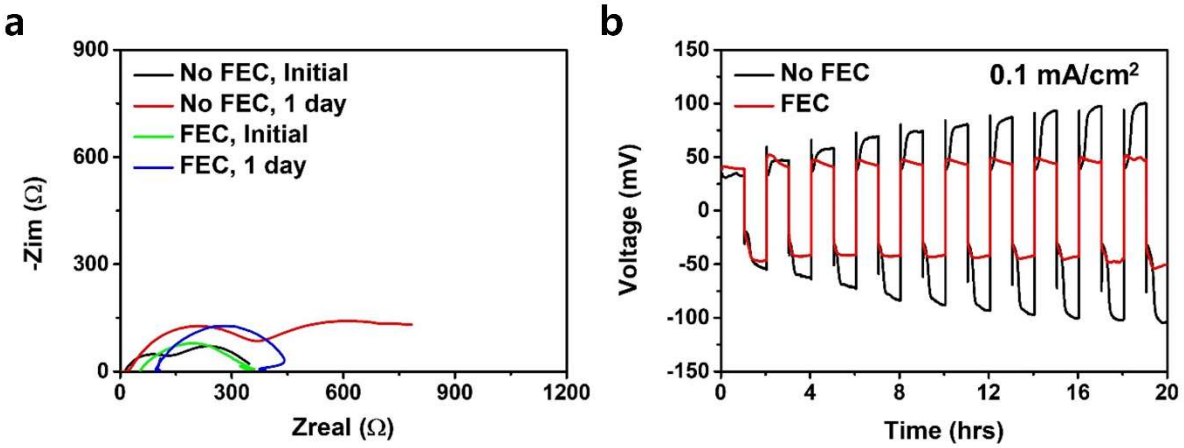

Fig. S6 The stabilized carbonate-based electrolytes upon 10 vol% fluorinated ethylene carbonate (FEC) addition. (a) The EIS measurements with and without FEC with 1M $NaClO_4$ salt and NaK liquid electrodes. (b) The Na metal stripping test with and without FEC shows that FEC stabilizes the NaK liquid electrodes and their electrode-electrolyte interfaces.

Note:

The EIS measurements were performed on coin cells incorporating $Na_{2+x}K$ electrodes incorporated in Cu foam. The measured impedances were overall lower than those observed with in-house thermogalvanic cells, possibly due to better electrode-electrolyte contact. The coin cells with FEC additives maintained similar charge transfer resistance and the impedance shape, while the coin cells without FEC additives resulted in extended charge transfer resistance and secondary circle in the impedance shape. The secondary impedance circle indicates the formation of potential electrode-electrolyte interphase layer with distinct diffusion characteristic.

During the Na metal stripping test, we observed continuous increase in overpotential during repeated cycles of Na deposition and stripping without FEC additives. The initial overpotential of approximately 45 mV with 0.1 mA/cm^2 current density increased to approximately 100 mV. With 10 vol% FEC additives, the overpotential was maintained at approximately 50 mV throughout the entire 20-hour Na deposition-stripping cycles. These results show that FEC additives stabilize the liquid metal electrode-liquid electrolyte interphase.

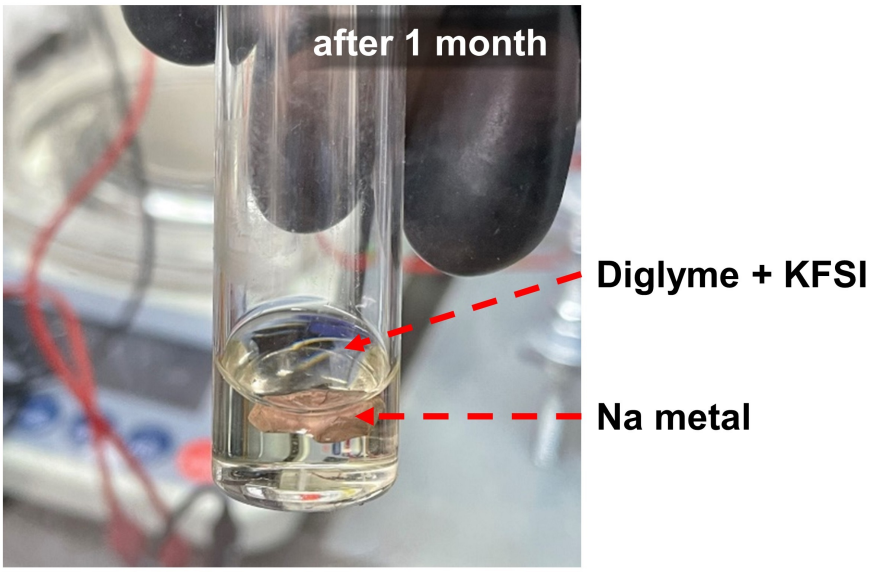

Fig. S7 Stable Na metal inside K^+ ion electrolyte consisting of DEGDME solvent and KFSI salts. Stable Na metal without signs of melting after 1 months indicates that the electrolyte does not lead to spontaneous Na^+ dissolution.

Note:

The stability of K^+ electrolyte was tested in terms of Na^+ ion dissolution from Na metal. A vial containing K^+ electrolytes (DEGDME with 2 M KFSI salt) and Na metal were allowed to rest for 1 month. If ion-exchange reaction occurred ($Na + K^+ \rightarrow Na^+ + NaK_x$), we were expecting notable shape change into spherical shape and partial melting of Na metal due to NaK_x formation at room temperature (NaK_x is semi-liquid at room temperature). After 1 month of exposure, we did not observe any partial melting of Na metal, indicating that the ion exchange reaction and dissolution of Na metal into the electrolyte did not occur. Instead, we observe brownish color change on some of the Na metal surface, indicating strong solid-electrolyte interphase (SEI) layer developing inside the electrolyte. The thin SEI layer is expected to stabilize the metal surface during repeated melting and solidification reaction inside the thermogalvanic cell, given that the morphological change is controlled to a reasonable degree inside the Cu-foam. The restricted dissolution of Na metal shows that the K^+ electrolyte can be safely used to observe the voltage signals arising from the chemical potential changes only of K element, not the mixture of Na and K chemical potentials.

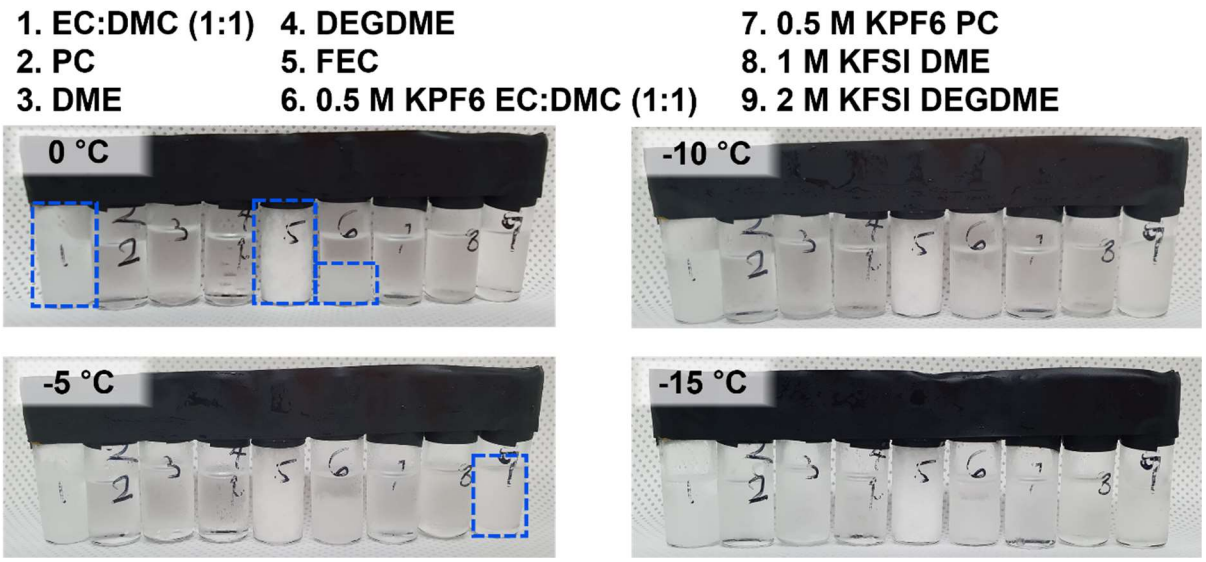

Fig. S8 The freezing tests of various solvents and Na^+ and K^+ electrolytes. The blue boxed regions indicate partially or completely frozen electrolytes.

Note:

Since we perform thermogalvanic tests from 4 ºC down to -15 ºC temperature, the solidification tests were performed on various electrolytes and solvents to optimize the electrolytes. We chose 5 different solvents (three carbonates and two glymes) and 4 salt-containing electrolytes for the freezing test. The results show that EC:DMC (1:1 volume ratio) and FEC freeze at 0 ºC among pure solvents and EC:DMC (1:1) with 0.5 M KPF6 electrolyte freezes among the electrolytes at 0 ºC. At -5 ºC temperature, we notice freezing behavior for DEGDME electrolyte with 2 M KFSI salt. The other electrolytes and solvents remained liquid even at -15 ºC temperature. Based on these results, we performed the eutectic composition tests with DME containing 1 M KFSI electrolyte down to -15 ºC, and the thermogalvanic tests down to 4 ºC with DEGDME containing 2 M KFSI-based electrolytes.

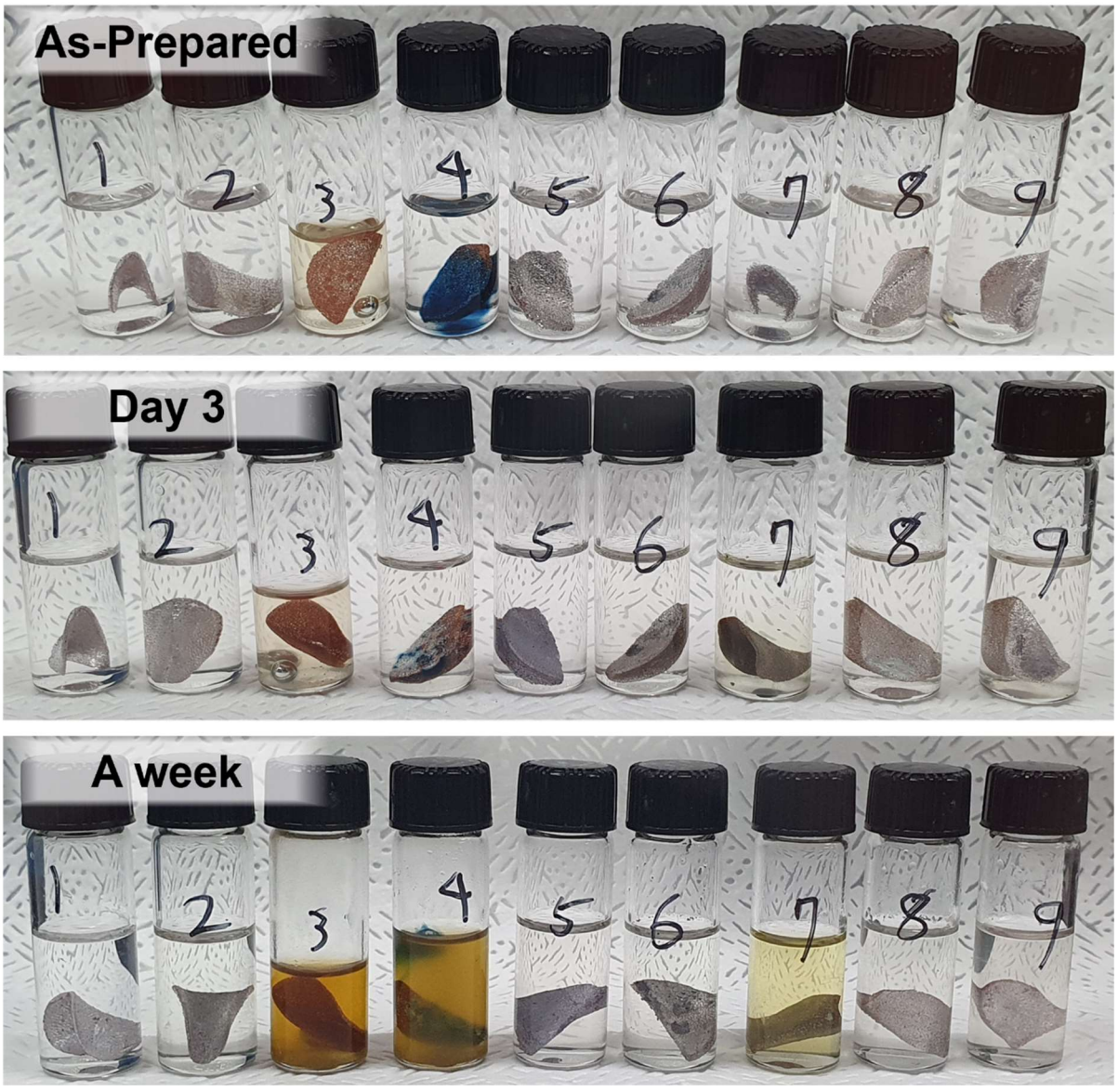

Fig. S9 The stability tests for the Cu foam-stabilized Na-K liquid metal electrodes inside various electrolytes. Labeled 1 to 9 indicates (1) pure EC:DMC=1:1 electrolyte (2) PC (3) DME (4) DEGDME (5) FEC (6) 0.5 M KPF_6 EC:DMC=1:1 (7) 0.5 M KPF_6 PC (8) 1 M KFSI DME (9) 2 M KFSI DEGDME. Only the electrolytes that do not result in excessive electrolyte degradation (0.5 M KPF_6 EC:DMC=1:1, 1 M KFSI DME and 2 M KFSI DEGDME) are employed in assessing the thermogalvanic performance across the phase transition regions.

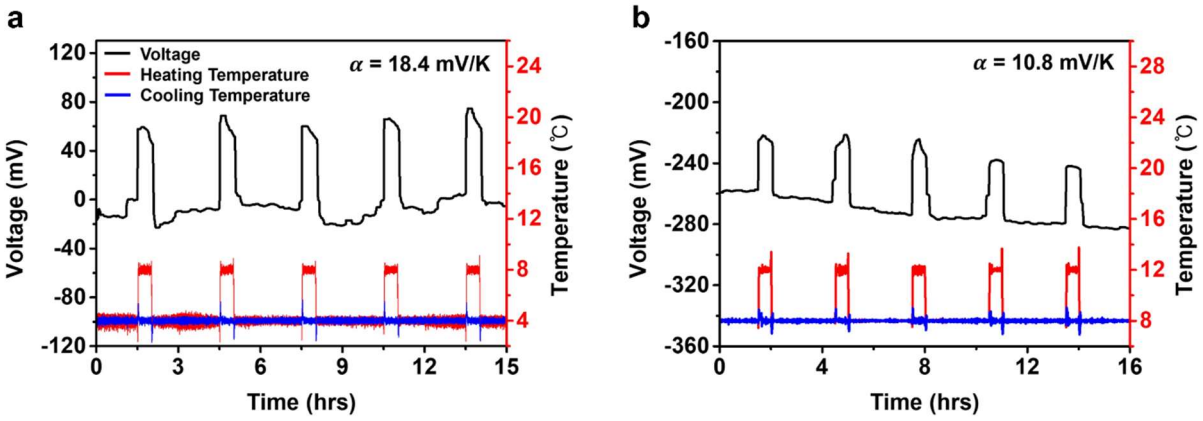

Fig. S10 The voltage measurements for thermogalvanic generators across. **a-b**, (**a**) 4-8 ºC temperature range and (**b**) 8-12 ºC temperature range with 2 M KFSI and 50 mM KNO_3 in DEGDME electrolyte.

Note:

The TGH employing $Na_{2+x}K$ electrodes and the K^+ only electrolyte generates a high thermopower of 18.4 mV/K and average thermal voltages of 73.6 mV across 4ºC – 8ºC temperature gradient. When operated between 8 ºC and 12 ºC in the liquid regime for K, the identical electrodes and electrolyte combination results in the generated voltage and thermopower of 43.2 mV and 10.8 mV/K, respectively. The observed thermopower for the solid-to-liquid phase transition regime is notably higher than that for the liquid regime, demonstrating the phase transition-driven thermopower enhancement.

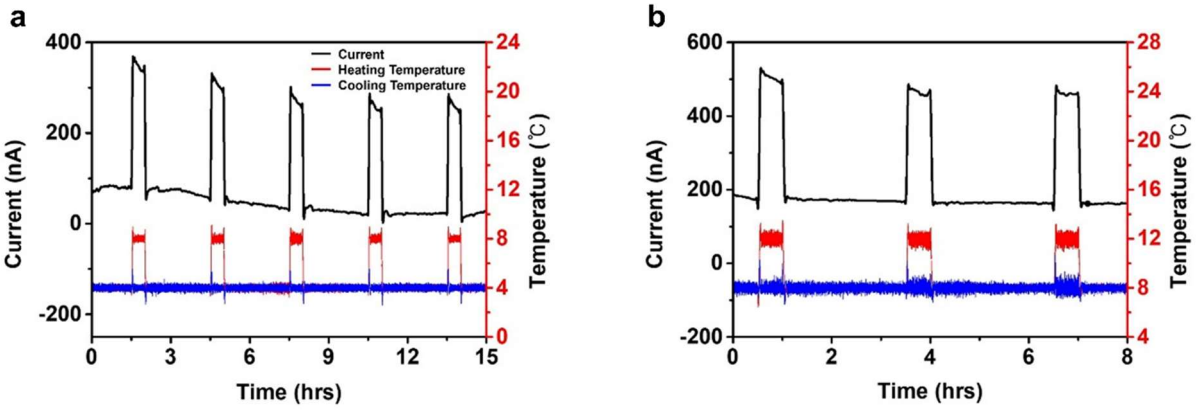

Fig. S11 Current measurements of thermogalvanic generators. **a-b**, The current measurements for thermogalvanic generators across (**a**) 4-8 ºC temperature range and (**b**) 8-12 ºC temperature range.

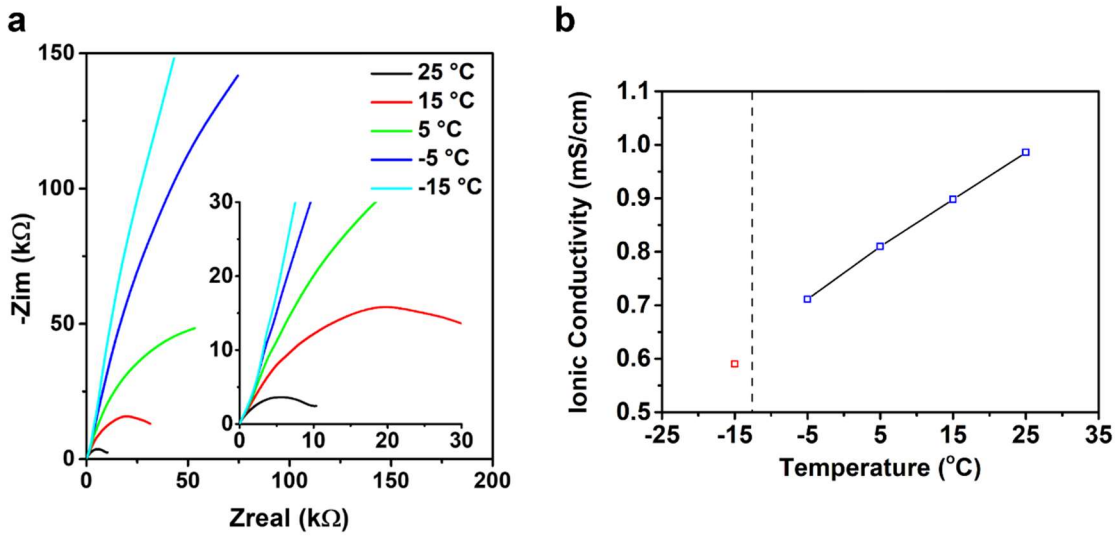

Fig. S12 EIS measurements of the TGH employing 2 M KFSI and 50 mM KNO_3 in DEGDME electrolyte at various temperatures. (a) The electrochemical impedance measurements of NaK-77 electrodes from 25 °C to -15 °C and (b) the resultant ionic conductivity. The red square indicates solid NaK-77 region and blue squares liquid NaK-77 region. The dash line indicates eutectic point (-12.6 °C).

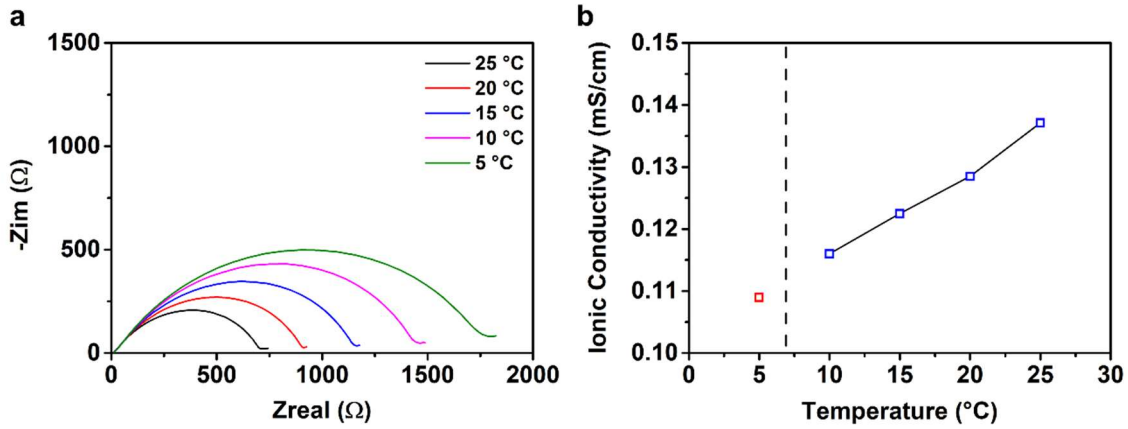

Fig. S13 EIS measurements of an optimized electrolyte employing 1M KPF_6 in DEGDME with 5% TTE and 20 mM $LiNO_3$, using $Na_{2+x}K$ symmetric electrodes. (a) The electrochemical impedance measured for $Na_{2+x}K$ electrodes at the temperatures from 25 ºC to 5 ºC at 5 ºC interval. The inset shows the zoomed-in view for the solution resistance. (b) The ionic conductivity of $Na_{2+x}K$ electrodes computed from the electrochemical impedance. The red square indicates solid NaK_2 region and blue squares liquid NaK_2 region. Dash line indicates solidus temperature (6.9 ºC).

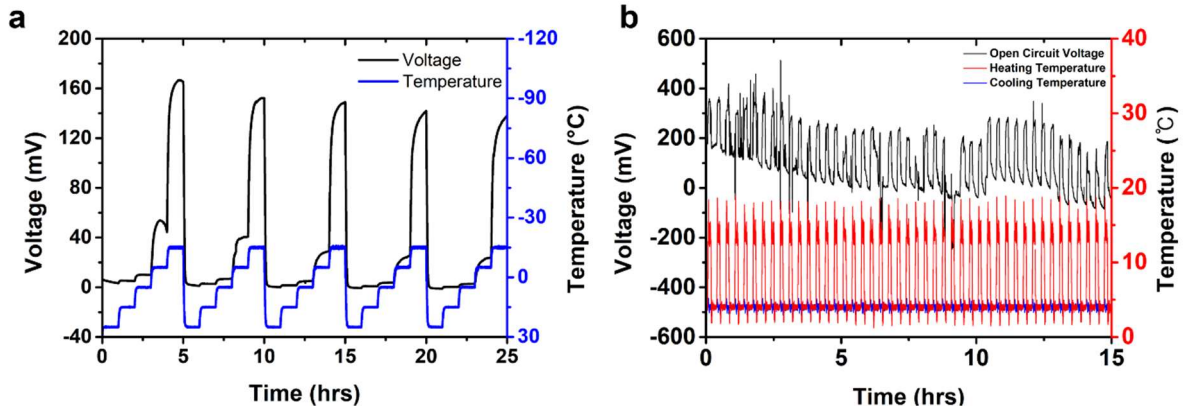

Fig. S14 Long-term stability test of the as-designed thermogalvanic energy harvesters. (a) The long-term stability tests in a coin-cell setup undergoing repeated temperature changes from 25 ºC to -15 ºC. The electrode undergoes direct liquid-to-solid phase transition at the eutectic temperature near -13 ºC. (b) The long-term stability tests as a thermogalvanic device under repeated spatial temperature gradient between 4 ºC and 14 ºC. The electrode undergoes partial liquid-to-solid phase transition at the solidus temperature around 7 ºC.

Note:

The results of the repeated solid-to-liquid phase transition are shown in Fig. S14. We found that the cells can be cycled without any significant change in voltage aspect or voltage level. In the thermally regenerative electrochemical cell (TREC) setup, the device was repeatedly cycled under 40 ºC temperature difference for five cycles over the course of 25 hours. The repeated solid-to-liquid phase transition occurred only for the NaK_2 alloy, and the morphological stability between the NaK_2 electrode and the copper foam was preserved during the cycles. In the thermogalvanic device setup, the device was repeatedly cycled under 10 ºC temperature gradient for 45 cycles. The slight voltage drop observed near 8^{th} hour was observed due to incomplete sealing issues of our in-house thermogalvanic cell and the resultant electrolyte evaporation. When the electrolyte was re-injected, stable voltage generation was observed during the following cycles. Based on these, we find that the long-term device output is reasonably maintained during the repeated cycling tests.

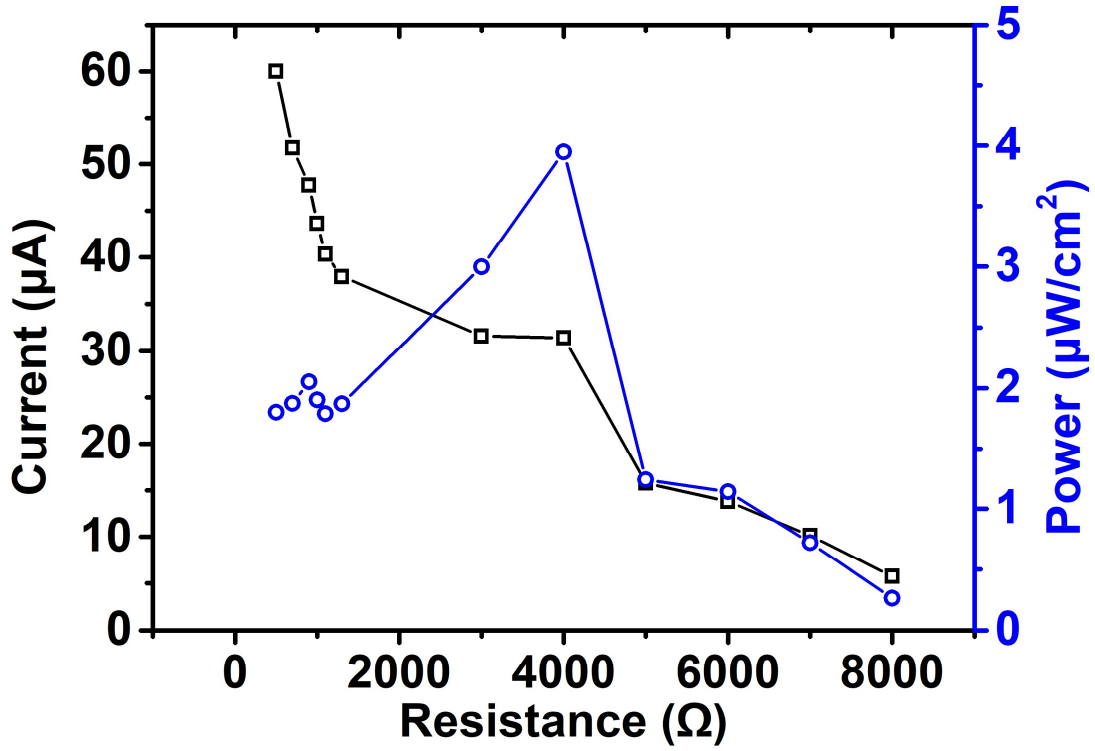

Fig. S15 The measured current and resultant power output of the TGH device according to the external resistance. The thickness of the electrode was 0.64 cm.

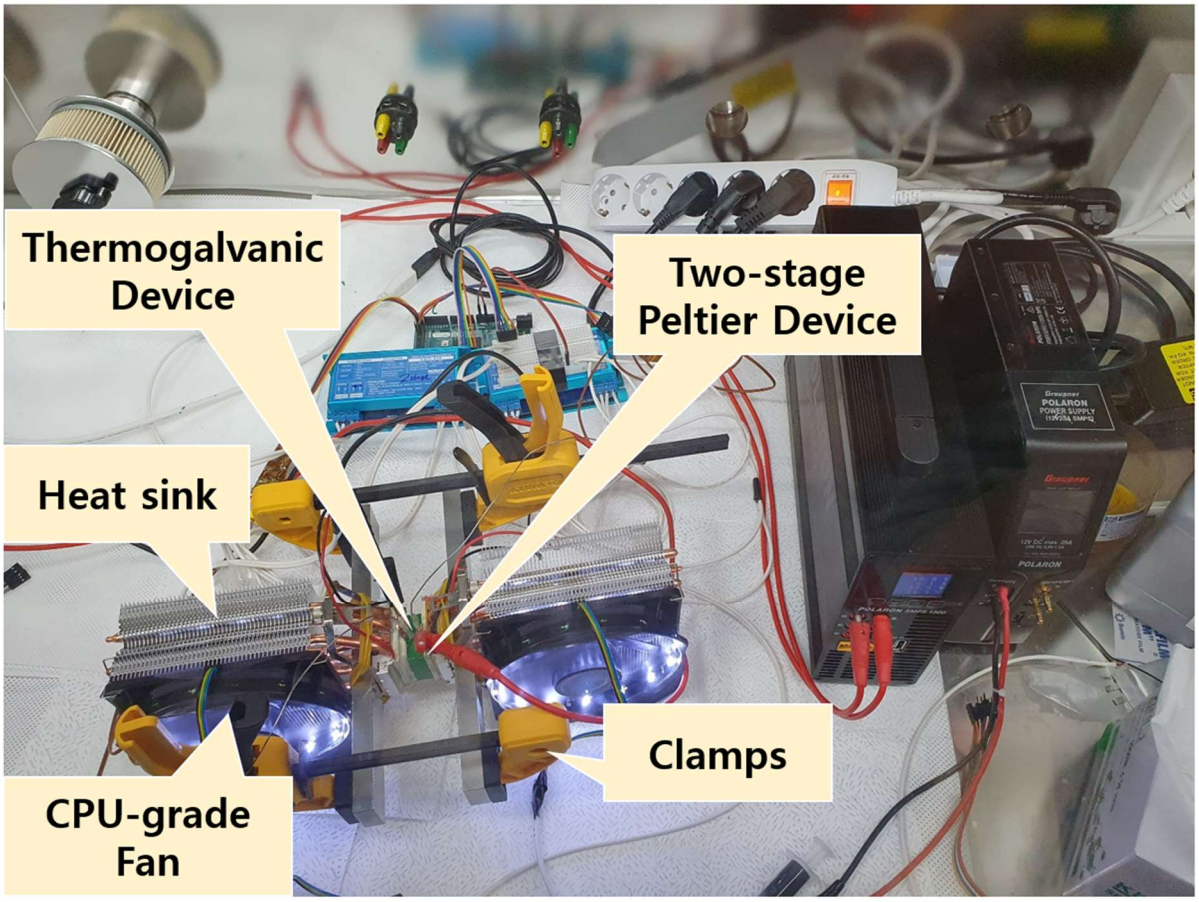

Fig. S16 The measurement setup for thermogalvanic devices with Na-K liquid metal electrodes targeting spatial temperature gradients. In-house thermogalvanic cells with polyethylene body is used with 1x1 cm^2 electrode area.

Note:

The in-house thermogalvanic devices were set up with copper blocks stable with sodium and potassium. Na-K alloys encapsulated in Cu foams were placed on these blocks, with a layer of electrolyte sandwiched between two electrodes. Polypropylene separators prevented short-circuiting, and insulated thermocouples measured core temperatures of Na-K electrodes for precise control via a feedback-loop algorithm. CPU-graded fans with large heat sinks ensured stable Peltier device performance.

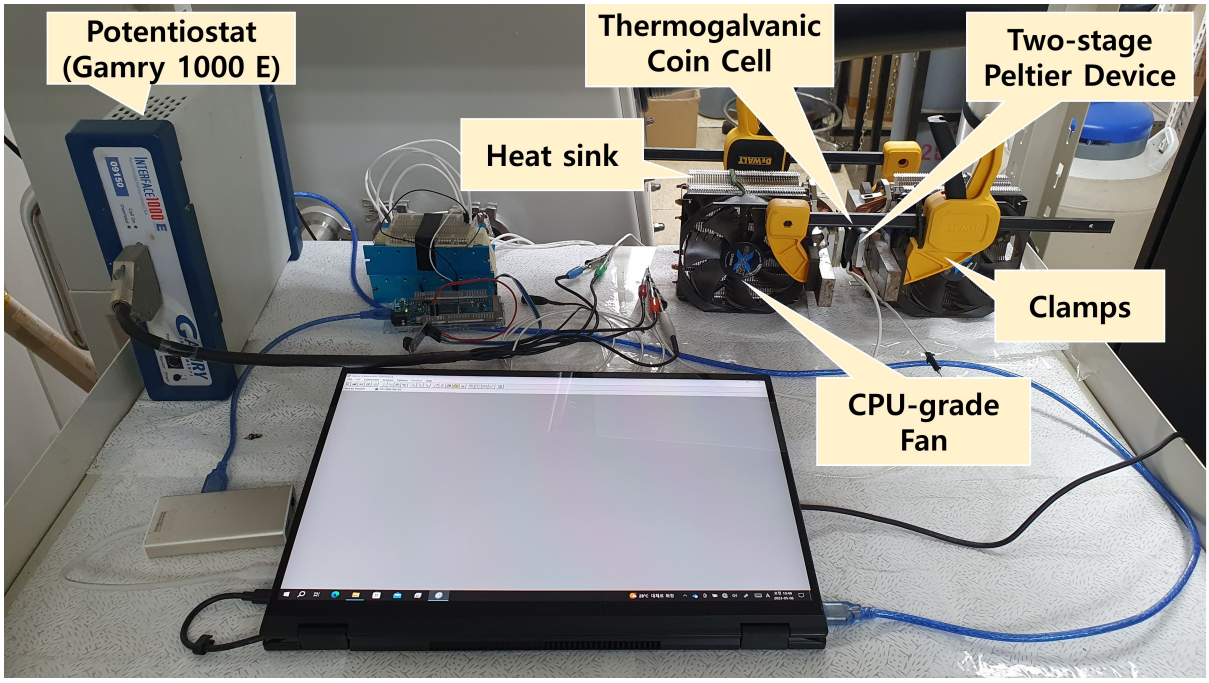

Fig. S17 The measurement setup for coin cell-based temporal thermal energy harvesters employing Na-K liquid metal electrodes.

Supplementary Note 1 | Thermodynamic model for phase transition-driven thermopower

The voltage generated in a thermogalvanic device scales directly with the chemical potential change of potassium in our device ($\Delta U = \frac{\Delta \mu_K}{e}$), and the chemical potential of potassium in one electrodes can be expressed as $\mu_{\mathrm{K}} = e_{\mathrm{K}} - Ts_{\mathrm{K}} + Pv_{\mathrm{K}}$, where e_{K}, T, s_{K}, P and v_{K} represent the partial molar internal energy, temperature, partial molar entropy, pressure and partial molar volume in the electrode, respectively. μ_{K} is a function of composition (x), phase (α), temperature (T) and pressure (P). We define a mechanochemical state $(\alpha, x_\alpha, P) \equiv \boldsymbol{M}$, and express the chemical potential as $\mu_{\mathrm{K}}\ (\boldsymbol{M}, T) = h_{\mathrm{K}}(\boldsymbol{M}) - Ts_{\mathrm{K}}$. Noting that $\left(\frac{\partial \mu_{\mathrm{K}}}{\partial T}\right)_P = -s_{\mathrm{K}}$ for a finite T, we can expand the chemical potential to the first order as the following:

$$\mu_{\mathrm{K}}\ (\boldsymbol{M}, T) = \mu_{\mathrm{K}}\ (\boldsymbol{M}, T_{\mathrm{ref}}) - (T - T_{\mathrm{ref}}) s_{\mathrm{K}}(\boldsymbol{M}, T_{\mathrm{ref}}) - O([T - T_{\mathrm{ref}}]^2)$$

The difference in chemical potential between two electrodes in our thermogalvanic device with hot-side liquid electrode ($\boldsymbol{M}_2$, T_2) and cold-side solid electrode ($\boldsymbol{M}_1$, T_1) can then be expressed as the following:

$$\Delta\mu_{\mathrm{K}}\ (\boldsymbol{M}, T) = \mu_{\mathrm{K}}\ (\boldsymbol{M_2}, T_2) - \mu_{\mathrm{K}}\ (\boldsymbol{M_1}, T_1)$$

Expanding the terms, we obtain the following relation for the power output to the leading order:

$$\Delta\mu_{\mathrm{K}} \approx \Delta\mu_{\mathrm{K}}^{\mathrm{o}}\ - \Delta T s_K(\boldsymbol{M_2}, 0) - T_1 \Delta s_K$$

where $\Delta\mu_{\mathrm{K}}^{\mathrm{o}} = \mu_{\mathrm{K}}\ (\boldsymbol{M_2}, T_{\mathrm{ref}}) - \mu_{\mathrm{K}}\ (\boldsymbol{M_1}, T_{\mathrm{ref}})$, $\Delta T = T_2 - T_1$ and $\Delta s_K = s_{\mathrm{K}}\ (\boldsymbol{M_2}, T_{\mathrm{ref}}) - s_{\mathrm{K}}\ (\boldsymbol{M_1}, T_{\mathrm{ref}})$. The first term mostly indicates the enthalpy difference between solid and liquid alloys, the second and third term arising from the entropy differences between two distinct phases.

In typical single component pure metal cases, we expect the first term (enthalpy of melting) and the third term (entropy differences multiplied by the cold-side temperature) to cancel out and the second term to dominate the voltage generation. In this scenario, the thermopower for solid-to-liquid phase transition may not exceed that for liquid-to-gas phase transition and we may expect lower thermopower from solid-to-liquid phase transition compared to the previously reported 9.9 mV/K thermopower from acetone to iso-propanol phase transition. Yet in the alloy systems of our demonstration, we note that the alloys undergo complex phase behavior upon cooling. At the composition $Na_{2+x}K$ just above the solidus temperature, the liquid phase follows the liquidus composition and is expected to be approximately $Na_{1.5}K$. This liquid undergoes direct solidification to Na_2K intermetallic compound. The entropy change from liquid mixture into a crystalline solid is expected to be complex. At the eutectic composition around NaK_2, the liquid NaK_2 undergoes phase separation into Na_2K+K as well as solidification. These complex phase behavior during liquid-to-solid phase transition is expected to contribute to the enhanced thermopower and makes it difficult to quantitatively predict the voltages generated in our device.

Supplementary Note 2 | The electrolyte effects on the thermopower measurements

The coin cells employing Na_2K and the eutectic NaK-77 are expected to show high thermopower when one of the two electrodes undergoes phase transition. For instance, when cycled between 4 and 20 ºC temperatures, the eutectic NaK-77 remains as liquid while Na_2K undergoes solidification. However, the observed thermopower only reaches 0.7 mV/K. In the temperature range -5 and -15 ºC, Na_2K remains as solid while NaK-77 undergoes eutectic solidification. With ether-based electrolyte, the observed thermopower in this case reaches 11.2 mV/K. These two experiments suggest two possibilities in optimizing electrolytes. Firstly, the ether-based electrolyte provides stable SEI for the phase-transforming electrode-electrolyte interface, allowing enhanced thermopower upon phase transition. Secondly, the experiments with Na_2K and NaK-77 electrodes tested between 4 and 20 ºC temperature range involves mostly liquid metal electrodes as both Na_2K and NaK-77 remains liquid above 7 ºC. Stabilizing liquid metal electrode-electrolyte interface may be critical to enhancing thermopower.

Based on the above hypotheses, $Na_{2+x}K$ electrodes were tested with various electrolyte combination in thermogalvanic devices between 4 and 8 ºC temperature range. Ether-based electrolytes were used in the experiments. When KFSI salt was mixed with KPF_6 salt, we observe that the measured thermopower decreases sharply. Employing KPF_6 alone also results in notably reduced thermopower. While it remains challenging to study the composition of SEI layers on liquid metal electrodes, it has been reported that KFSI salt builds more stable SEI layer than KPF_6 salt[1] protecting K metal electrodes. We expect this to be also true on our thermogalvanic device, making it difficult to stabilize the SEI layers on the electrode.

In the battery community, employing solvent additive containing halide ions has been reported, in efforts to replace salts with low ionic conductivity. The addition of fluorinated ethylene carbonate (FEC) to carbonate-based solvents (EC) is an example. Since our experiments involve temperatures below room temperature, strong ionic conductivity was required even at -15 ºC. It has been reported that KPF_6 salt in ether-based electrolytes enable high ionic conductivity even at low temperature[2] and we chose to include TTE to the electrolyte along with KPF_6 salts. Adding TTE additives to the electrolyte, in efforts to increase the inorganic portion of the SEI, indeed increased the measured thermopower and we attribute the increase to the stabilized SEI layer. Eventually, the optimized combination employing KPF_6 salt, ether-based solvent and TTE additives are obtained.

Supplementary Materials References

1 H. Wang, D. Yu, X. Wang, Z. Niu, M. Chen, L. Cheng, W. Zhou and L. Guo, *Angewandte Chemie International Edition*, 2019, **58**, 16451–16455.

2 J. Chen, D. Yu, Q. Zhu, X. Liu, J. Wang, W. Chen, R. Ji, K. Qiu, L. Guo and H. Wang, *Advanced Materials*, 2022, **34**, 2205678.